

Determination of unique Feature set for AM Bitewing Dental Radiographs as a Bio-metric information

Shaishavkumar Parmar¹ Mehul Amin²

^{1,2}Assistant Professor, Dept. of ECE

^{1,2}Dr. Jivraj Mehta Institute of Technology, Mogar, Anand, India

Abstract—Recent growth in the number of studies for automating the process of post-mortem (PM) identification of deceased individuals based on various features of teeth is remarkable. Hence, nowadays dental X-ray has played an important role in human identification. Particularly, in cases of severe accidents (Airplane crashes, 9/11 bombing, Car/Train accidents), natural disasters (Asian Tsunami, Flood, Earthquake, Volcanic eruption, Typical cyclone), etc. wherein other identification clues like fingerprint, iris, face, etc. are not available for human identification. Dental features remain less invariant over longer time period. The purpose of dental image processing is to match the post-mortem (PM) radiograph with the ante-mortem (AM) radiograph based on some features of the dental X-ray images. The dental radiograph images acquired may be of poor quality and contrast. Therefore, first it is important to classify and then enhance the quality of image and thereafter applied various segmentation algorithms on enhanced dental radiograph image. Various features of individual tooth are being extracted and identification can be possible based on matching of these feature vectors for PM images which are calculated and compared with AM images. This paper provides a basic idea of various classification, enhancement, segmentation and detail feature extraction techniques for human identification using dental radiographs.

Keywords: Dental Identification System (DIS), Dental Radiograph, Gap Vally, Region of Interest (ROI),

I. INTRODUCTION

Biometric systems play an important role in identifying individuals based on some physiological and behavioral characteristics such as fingerprints, face, hand geometry, iris, voice, and signature[7]. While most of these characteristics were not suitable for post-mortem (PM) identification, especially under the severe circumstances usually in mass disasters (e.g., airplane crashes, 9/11 bombing, Asian tsunami[5]). Hence, for human identification system dental radiograph was one of the best avenues because teeth were not only highly resistant to decomposition, but were also unique to an individual [12]. Also teeth being the hardest and the most impregnable parts of human body were thus regarded as the best candidates for human PM identification [14].

A bitewing image includes the features of both jaws signifying bite and holds more information about the curvature and the roots. While periapical images include only a single jaw either upper jaw called as upper periapical image or lower jaw called as lower periapical image to obtain the tip of the root and surroundings tissues. Panoramic images include features of both jaws including

sinuses, nasal area, etc. that do not show fine details as do bitewing and periapical. Hence, for most dental image processing bitewing images are preferred.

A. Image Enhancement

Dental radiograph consists of three regions namely background area (having lowest intensity), bone area (having average intensity) and teeth areas (having highest intensity). Sometimes the intensity of bone area and teeth area are nearly same. So, for abundant feature extraction, the teeth area should be identified from bone area [14].

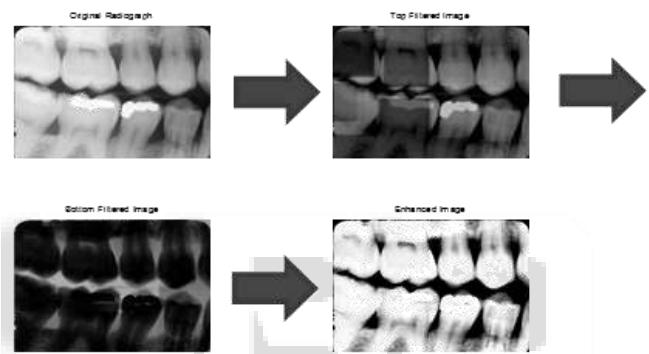


Fig. 1: Image Enhancement Process

B. Image Segmentation

Now, dental radiograph segmentation is performed which includes separating upper and lower jaw and thereafter separating each individual tooth.

C. Feature Extraction

Feature extraction process follows tooth segmentation wherein some specific features are defined which are further used for matching post-mortem (PM) images with ante-mortem (AM) images.

There are many features available in literature for comparing AM and PM dental radiograph images. The features are used solely for comparing the radiographs i.e. identification purposes. In this paper we extract many geometrical features of individual tooth namely: teeth area (%), major axis length, minor axis length, Eccentricity, perimeter, four properties of Gray level co-occurrence matrix (GLCM) as combined features, compactness, Fourier descriptors, and Skeleton.

II. RADIOGRAPH ENHANCEMENT

The dental radiograph images acquired may be of poor quality and contrast. Therefore, first it is important to enhance the quality of image. Most image enhancement operations are applied to make the image visually more appealing. This can be accomplished by increasing contrast, optimizing brightness and reducing un-sharpness and noise.

If the intensity value of the pixel is larger than the average intensity values of its neighbors, then it is classified as a tooth pixel, otherwise it is classified as background. To separate each tooth region, we apply a binary morphological top hat and bottom hat filtering operation to eliminate small noisy parts and smooth the teeth regions. Then, we subtract the teeth areas from the original image to obtain the bones and the background regions, and apply simple thresholding to separate the bones from the background.

III. RADIOGRAPH SEGMENTATION AND TEETH SEPARATION

The goal of radiograph segmentation is to localize the region of each tooth in a dental X-ray image. Dental radiographs may suffer from poor quality, low contrast and uneven exposure that complicate the task of segmentation. Dental X-ray images have three different regions: soft tissue regions and background with the lowest intensity values, bone regions with average intensity values, and teeth regions with the highest intensity values. In some cases the intensity of the bone areas is close to the intensity of the teeth, which makes it difficult to use a single threshold for segmenting the entire image.

In this paper, after enhancing teeth from background, each tooth is separated from its surroundings in order to prepare for feature extraction. This is achieved by first separating upper and lower jaws, and then separating each tooth.

A. Separating the upper and lower jaws

If we consider the image in fig, it is clear that a horizontal or a near horizontal line can separate upper and lower jaws. This can be achieved by using horizontal integral projection as follows.

Let $f(i, j)$ be the $r \times c$ grayscale image obtained from the enhancement stage, the horizontal integral projection is

$$H(i) = \sum_{j=1}^c f(i, j)$$

Due to grayscale variation, we normalize the line by median values.

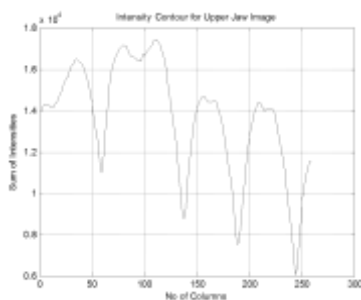


Fig. 2: Intensity contour for upper jaw image
Locating deep points

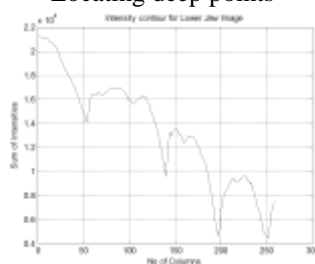


Fig. 3: Intensity contour for lower jaw image
Locating deep points



Fig. 4: Upper jaw X ray of original x-ray

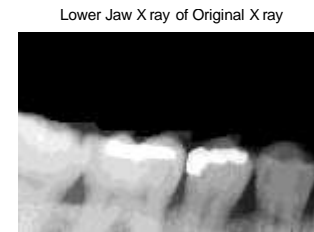


Fig. 5: Upper jaw X ray of original x-ray

B. Separating each individual tooth

To separate each individual tooth we use a technique similar to the one used for separating the jaws. The goal is to find the lines that separate adjacent teeth. This can be achieved by using the integral projection method in the vertical direction. If $f(i, j)$ is the $r \times c$ grayscale image obtained from the segmentation stage, the vertical projection is

$$V(i) = \sum_{j=1}^r f(i, j)$$

The separating lines are located by finding valleys in the result of the vertical projection. From those valleys in the projection curves we separate each individual tooth. For each projection, we use a threshold value to obtain the valleys that identify locations of vertical lines between adjacent teeth.

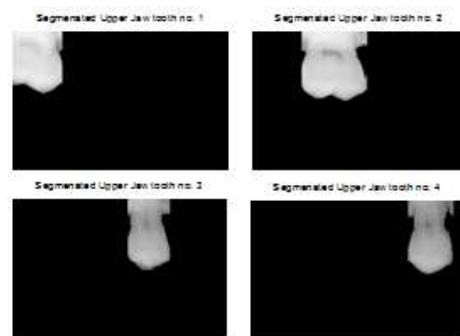


Fig. 6: Segmentation of Upper jaw's tooth

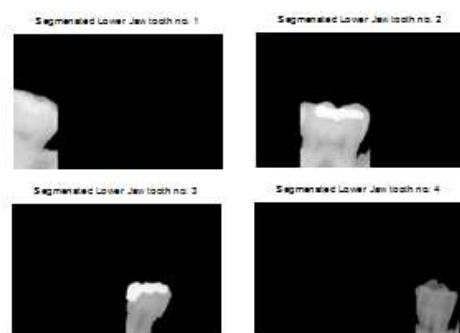


Fig. 7: Segmentation of Lower jaw's tooth

IV. FEATURE EXTRACTION

Feature extraction is used prior to matching the AM and PM images. Some unique features of the tooth are extracted which can be any of crown contour, root contour, tooth contour, contours of dental work, shape model and shape analysis (PCA), etc.

A. Tooth Area:

The actual number of pixels in the region. (This value might differ slightly from the value returned by *bwarea*, which weights different patterns of pixels differently.)

B. Major axis length :

The length (in pixels) of the major axis of the ellipse that has the same normalized second central moments as the region. This property is supported only for 2-D input label matrices.

C. Minor axis length

The length (in pixels) of the minor axis of the ellipse that has the same normalized second central moments as the region. This property is supported only for 2-D input label matrices.

D. Eccentricity:

The eccentricity of the ellipse that has the same second-moments as the region. The eccentricity is the ratio of the distance between the foci of the ellipse and its major axis length. The value is between 0 and 1.

E. Orientation:

The angle (in degrees ranging from -90 to 90 degrees) between the x-axis and the major axis of the ellipse that has the same second-moments as the region. This property is supported only for 2-D input label matrices.

F. Gray-level co-occurrence matrix

A statistical method of examining texture that considers the spatial relationship of pixels is the gray-level co-occurrence matrix (GLCM), also known as the gray-level spatial dependence matrix [13]. The GLCM functions characterize the texture of an image by calculating how often pairs of pixel with specific values and in a specified spatial relationship occur in an image, creating a GLCM, and then extracting statistical measures from this matrix.

1) Energy:

It is also known as uniformity or the angular second moment. It returns the sum of squared elements in the GLCM. It is defined for an image *C* as follows

$$\text{Energy} = \sum_{i,j=1}^N C_{i,j}^2$$

Energy is 1 for a constant image

2) Contrast:

It measures the local variations in the gray-level co-occurrence matrix. It returns a measure of the intensity contrast between a pixel and its neighbour over the whole image.

$$\text{Contrast} = \sum_{i,j=1}^N (i-j)^2 C_{i,j}^2$$

Contrast is 0 for a constant image.

3) Correlation:

It measures the joint probability occurrence of the specified pixel pairs. It returns a measure of the intensity contrast between a pixel and its neighbour over the whole image.

$$\text{Correlation} = \frac{\sum_{i,j=1}^N (i-\mu_i)(j-\mu_j)C_{i,j}^2}{\sigma_i \sigma_j}$$

Correlation is 1 or -1 for a perfectly positively or negatively correlated image.

4) Homogeneity:

It measures the closeness of the distribution of elements in the GLCM to the GLCM diagonal. It is defined as

$$\text{Homogeneity} = \sum_{i,j=1}^N \frac{C_{i,j}}{1+|i-j|}$$

Homogeneity is 1 for a diagonal GLCM

5) Perimeter:

p-element vector containing the distance around the boundary of each contiguous region in the image, where p is the number of regions.

6) Fourier Descriptors (FD):

FD's are powerful for 2-dimensional shape description. Fourier descriptors are given by

$$F(u, v) = \frac{1}{mn} \sum_{k=0}^{N-1} \sum_{l=0}^{N-1} c(x, y) e^{-2\pi i (\frac{kx}{m} + \frac{ly}{n})}$$

Where, (m, n) is size of the image is, *N* is number of Fourier descriptors and $c(x, y)$ represents the image. The Coefficients $F(u, v)$ are called Fourier Descriptors (FD). They represent discrete contour of a shape in Fourier domain. Fourier Descriptors are often used to smooth out fine details of shape and also for template matching.

7) Compactness:

It is a measure of efficiency of a contour to contain a given area.

8) Skeleton:

An important approach for representing the spectral shape of a planner region is to reduce it to a graph. This reduction may be accomplished by obtaining the skeleton of the region via a thinning (also called skeletonising) algorithm.

The skeleton of a region may be defined via the medial axis transformation (MAT). The MAT of a region *R* with border *b* is as follows. For each point *p* in *R*, we find its closest neighbour in *b*. If *p* has more than one such neighbour, it is said to belong to the medial axis (skeleton) of *R*.

Step:1 Iteratively compute $f^k(x, y)$ as follows until $f^k(x, y) = f^{k-1}(x, y)$:

$$f^k(x, y) = f^0(x, y) + \min(f^{k-1}(p, q))$$

$$\forall (p, q) \text{ Such that } d((x, y), (p, q)) \leq 1$$

Step: 2 Medial axis is given by all points such that

$$f^k(x, y) \geq f^k(p, q)$$

$$\forall (p, q) \text{ Such that } d((x, y), (p, q)) \leq 1$$

V. RESULTS AND DISCUSSION

In this study, the experimental setup consists of Windows 7 ultimate operating system, Intel(R) Core(TM) i5-2410M CPU, 2.30 GHz Processor PCs having 4 gigabytes of memory (RAM) and 32-bit operating system. The optimization algorithm was implemented by the MATLAB,

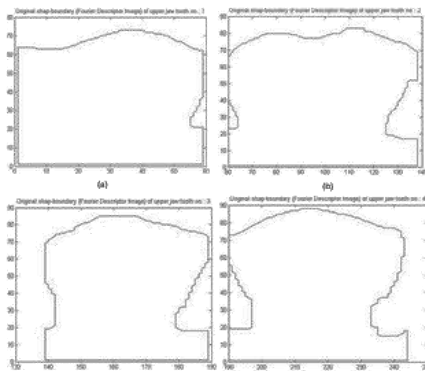


Fig. 8: Fourier descriptor of each Tooth of Upper jaw

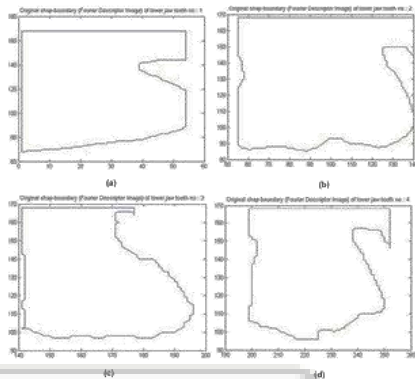


Fig. 9: Fourier descriptor of each Tooth of lower jaw

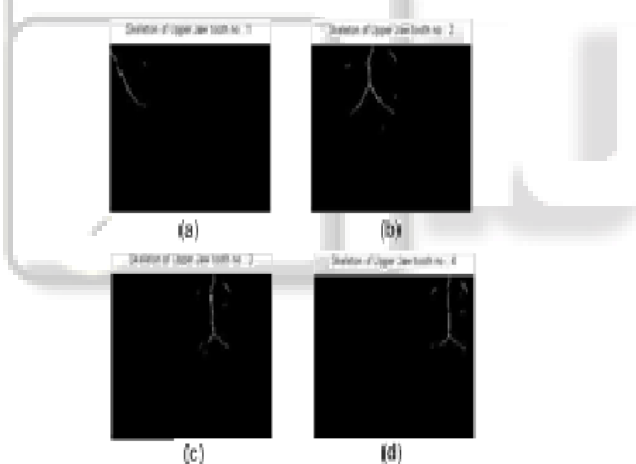


Fig.10: Skeleton of each tooth of Upper jaw

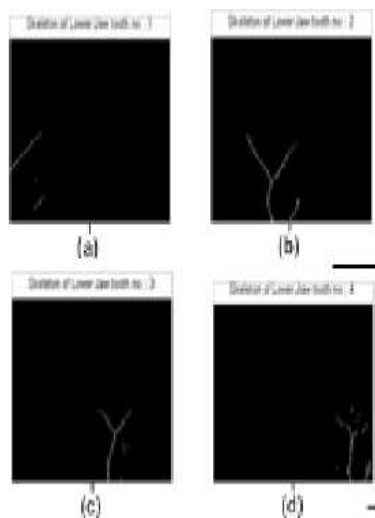


Fig. 11: Skeleton of each tooth of Lower jaw

The Language of Technical Computing using version of 7.5.0.342 (R2007b) licenced by The Math works Inc.

In general, initial stage of human identification or diagnosis system is classification of dental images. Here in our experiment, we used bitewing dental images among from three types of classifications. So, no need to perform any further consideration for classification of dental images.

Primarily, from poor quality of dental radiograph, to get exact parameters for diagnosis of teeth or identification of human based on teeth, we performed morphological operation on dental radiograph to enhance or proper visibility of teeth. For that we used square structuring element to perform morphological operation.

Features	Upper Jaw				Lower Jaw			
	Tooth 1	Tooth 2	Tooth 3	Tooth 4	Tooth 1	Tooth 2	Tooth 3	Tooth 4
Area (%)	9.0366	13.231	8.6091	9.1768	0.2597	0.37691	0.17466	0.30336
Major Axis length	79.109	92.406	95.46	98.726	170.23	159.63	105.48	110.25
Minor Axis length	66.003	84.9	53.803	56.177	64.242	107.3	58.753	72.847
Orientation	82.596	78.273	88.814	89.499	89.379	77.655	90	89.431
Eccentricity	1.1986	1.0884	1.7743	1.7574	2.6499	1.4877	1.7952	1.5134
Contrast	[0.1618 0.1974]	[0.2666 0.4062]	[0.1800 0.3904]	[0.2028 0.4380]	[0.2005 0.2292]	[0.2826 0.4721]	[0.2279 0.3586]	[0.2074 0.4017]
Correlation	[0.9799 0.9754]	[0.9763 0.9641]	[0.9767 0.9497]	[0.9752 0.9467]	[0.9792 0.9761]	[0.9774 0.9623]	[0.9645 0.9444]	[0.9686 0.9397]
Energy	[0.8237 0.8328]	[0.7653 0.7606]	[0.8392 0.8336]	[0.8294 0.8232]	[0.8994 0.8012]	[0.7401 0.7344]	[0.8664 0.8610]	[0.8613 0.8558]
Homogeneity	[0.9971 0.9946]	[0.9952 0.9927]	[0.9967 0.9930]	[0.9996 0.9921]	[0.9964 0.9959]	[0.9949 0.9915]	[0.9995 0.9936]	[0.9996 0.9928]
Perimeter	125	224	211	234	149	274	206	383
Compactness	0.99273	0.99669	0.99757	0.99789	0.99985	0.99994	0.99995	0.99997
Fourier Descriptor	8006	11313	9498	10199	36874	44670	31003	36024
Skeleton	57	122	105	109	46	145	99	117

Table 1: Features of the Dental Radiograph

REFERENCES

- [1] H. Chen, S. Minut Jain A.K, "Dental Biometrics: Human Identification Using Dental Radiographs", in International Conference on Audio and Video-based Biometric Person Authentication (AVBPA), Guildford, UK, June 2003, pp. 429-437.
- [2] Jain A.K and Hong C, "Matching of dental X-ray images for human identification", The Journal of Pattern Recognition Society, pp. pp: 1519-1532, Dec 2003.
- [3] Hong C and Jain A.K, "Tooth Contour Extraction for Matching Dental Radiographs" in International Conference on Pattern Recognition (ICPR'04), vol. Vol 3, Cambridge, UK, Aug 2004, pp. pp: 522-525.
- [4] Nomir O and Abdel-Mottaleb M, "A system for human identification from X-ray dental radiographs" The Journal of Pattern Recognition, pp. 1295-1305, December 2005.
- [5] Hong C and Jain A.K, "Dental Biometrics: Alignment and Matching of Dental Radiographs" in IEEE Transactions on Pattern Analysis and Machine Intelligence (PAMI), vol. 27, Augus 2005, pp. 1319-1326.
- [6] Antti Vanne, Samuli Siltanen, Seppo Jarvenpaa, Jari P. Kaipio, Matti Lassas and Martti Kalke Ville Kolehmainen, "Parallelized Bayesian Inversion for Three-Dimensional Dental X-ray Imaging" in IEEE Transactions on Medical Imaging, vol. 25, pp. 218-228.
- [7] DiaaEldin M. Nassar, Gamal Fahmy and Hany H. Ammar Eyad Haj Said, "Teeth Segmentation in Digitized Dental X-Ray Films Using Mathematical Morphology" in IEEE Transactions on Information Forensics and Security (IFS), vol. 1, June 2006, pp. 178-189.
- [8] Nomir O and Abdel-Mottaleb M, "Hierarchical contour matching for dental X-ray radiographs" The Journal of Pattern Recognition, pp. 130-138, May 2007.
- [9] Nomir O and Abdel-Mottaleb M, "Human Identification from Dental X-Ray Images Based on the Shape and Appearance of the Teeth" in IEEE Transactions on Information Forensics and Security (IFS), vol. 2, June 2007, pp. 188-197.
- [10] Nomir O and Abdel-Mottaleb M, "Fusion of Matching Algorithms for Human Identification Using Dental X-Ray Radiographs" in IEEE Transaction on Information Forensics and Security (IFS), vol. 3 Issue: 2, June 2008, pp. 223-233.
- [11] S. S. Brilliant, D. Primeaux and K. Najarian, G. F. Olsen, "An Image-Processing Enabled Dental Caries Detection System" in ICME International Conference on Complex Medical Engineering, 2009 (CME), Tempe, AZ, April 2009, pp. 1-8.
- [12] Mehnert A, Mahoney M, Crozier S Tohnak S, "Dental identification system based on unwrapped CT images" in IEEE International conference on Engineering in Medicine and Biology Society (EMBC), Minneapolis, Sept 2009, pp. 3549-3552.
- [13] O. Gormez and H.H. Yilmaz, "Image Post-Processing in Dental Practice" European Journal of Dentistry, pp. 343-347, October 2009.
- [14] Chun-Hung Kuo and Phen-Lan Lin, "An effective dental work extraction and matching for bitewing radiographs" in IEEE International Conference on International Computer Symposium (ICS), Tainan, December 2010, pp. 495-499.
- [15] Raju J and Modi C.K, "A Proposed Feature Extraction Technique for Dental X-Ray Images Based on Multiple Features" in IEEE International Conference on Communication Systems and Network Technologies (CSNT), Katra, Jammu, June 2011, pp. 545-549.
- [16] Ghodsi S.B and Faez K, "A novel approach for matching of dental radiograph image using Zernike moment" in IEEE International Conference on Computer Science and Automation Engineering (CSAE), vol. 3, Zhangjiajie, May 2012, pp. 303-306.
- [17] H. Hakim, N. Motahir, P. Yousefi and M. M. Hossini B. Yousefi, "Visibility Enhancement of Digital Dental X-Ray for RCT Application Using Bayesian Classifier and Two Times Wavelet Image Fusion", Journal of American Science, vol. 8, no. 1, pp. 7-13, 2012.
- [18] Desai N.P, Modi C.K Prajapati D.B, "A Simple and Novel CBIR Technique for Features Extraction Using AM Dental Radiographs" in IEEE International Conference on Communication Systems and Network Technologies (CSNT), Rajkot, May 2012, pp. 198-202.
- [19] R. Thanki and D. Trivedi, "Introduction of Novel Tool for Human Identification Based on Dental Image Matching", International Journal of Emerging Technology and Advanced Engineering, vol. 2, Issue: 10, pp. 399-402, October 2012.

BOOKS

- [20] Richard E. Woods, Steven L. Eddins Rafael C. Gonzalez, Digital Image Processing using MATLAB, 2nd ed. New Delhi: Tata McGraw Hill Education, 2011.
- [21] Anil K. Jain, Fundamentals of Digital Image Processing.: Prentice Hall of India, 2002.
- [22] Rudra Pratap, Getting Started with MATLAB 7. New York: Oxford University Press, 2006.